

含铁氧体片的脊形和槽形波导的准TE_{m0}模解

宗卫华, 余显烨, 梁昌洪

(西安电子科技大学工程学院, 陕西西安 710071)

摘要: 用模式匹配法精确分析铁氧体片对称放置的脊形和槽形波导的准TE_{m0}模, 并对几种特殊情形进行计算, 结果与文献吻合. 进一步计算结果表明含铁氧体片的脊形波导具有宽频带特性, 含铁氧体片的槽形波导具有较大相位移. 由于考虑了高次模, 此方法较目前文献提及的方法更为精确.

关键词: 铁氧体; 脊形波导; 槽形波导; 移相器; 模式匹配法

中图分类号: TN623 **文献标识码:** A **文章编号:** 0372-2112 (2002) 06-0811-04

Solution of Quasi-TE_{m0} Mode in Ferrite Slabs Loaded Ridged and Grooved Waveguides

ZONG Wei-hua, SHE Xian-ye, LIANG Chang-hong

(School of Electronic Engineering, Xidian University, Xi'an, Shaanxi 710071, China)

Abstract: A mode matching method is used to accurately analyze the quasi-TE_{m0} mode in ferrite slabs symmetrically loaded ridged and grooved waveguides. Numerical results are identical to those in the references. Further computation indicates that the ferrite slabs loaded ridged waveguide has broadband frequency properties and the grooved waveguide has greater differential phase shift. With higher modes considered, this method is superior to those in literatures published in recent years.

Key words: ferrite; ridged waveguide; grooved waveguide; phase shifter; mode matching method

1 引言

铁氧体移相器是相控阵技术中重要的一种微波元件, 精确地进行设计已引起很多学者的注意. 槽形波导铁氧体环形锁式移相器由于其价值高、功率容量大, 在很多系统中得到应用. M Okniewski^[5]用模式匹配方法分析了含有圆柱形铁氧体片的复杂形状波导的特性, 而关于填充铁氧体片的槽形波导铁氧体移相器迄今没有精确的场分析. 本文用模式匹配方法得到含铁氧体片和多介质片的脊形波导和槽形波导的传输模式, 计算结果与文献[1, 2]比较吻合. 由于考虑了高次模, 此方法较文献[3]更精确. 这对于研究铁氧体移相器的传输模式、频率特性和移相特性, 改进非互易铁氧体移相器的性能具有重要意义.

2 计算模型及公式

2.1 移相器模型

图1、图2分别给出了含铁氧体片的脊形、槽形波导的理论模型. 区域1为铁氧体(相对介电常数 ϵ_1), 区域2为空气, 区域3为介质(相对介电常数 ϵ_3), 这是目前通用的铁氧体环形移相器的两种模型.

2.2 场分布

设电磁波沿Z轴传播, 因子为 $e^{-j\beta z}$, β 为相位常数. 区域

1, 铁氧体磁化方向为y, 工作于剩磁状态, 磁导率张量 μ

$$\mu = \mu_0 \begin{bmatrix} 1 & 0 & \pm j\kappa \\ 0 & 1 & 0 \\ \mp j\kappa & 0 & 1 \end{bmatrix}$$

其中 κ 代表顺时针磁化, $-\kappa$ 代表逆时针磁化.

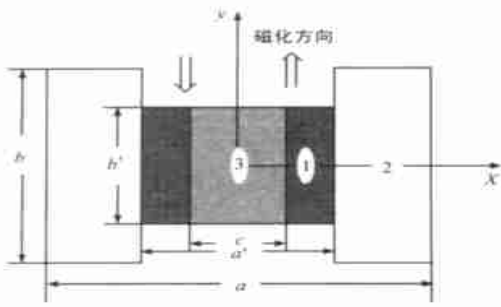
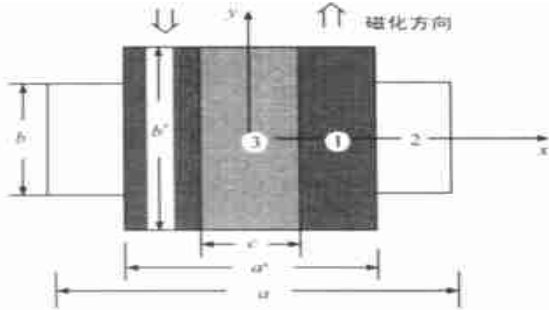
波导中传输模式为混和模, 可写为一个正弦变化的基模与多个高次凋落模的线性组合. 当 $a > b, b'$ 时, 主模为准TE₁₀模(基模为TE₁₀模), 本文仅给出准TE_{m0}模(基模为TE_{m0}模)的场分布(为书写方便省略 $e^{-j\beta z}$ 及 $e^{j\omega t}$ 项).

区域1:

$$E_{y1} = A_{01}^{(1)} \cos(k_{x0}^{(1)} x) + A_{01}'^{(1)} \sin(k_{x0}^{(1)} x) + \sum_{l=1}^{\infty} [A_{l1}^{(1)} \text{ch}(\Gamma_{l1}^{(1)} x) + A_{l1}'^{(1)} \text{sh}(\Gamma_{l1}^{(1)} x) + A_{l1}^{(2)} \text{ch}(\Gamma_{l1}^{(2)} x) + A_{l1}'^{(2)} \text{sh}(\Gamma_{l1}^{(2)} x)] \cos(k_{y1} y)$$

$$H_{y1} = \sum_{l=1}^{\infty} [B_{l1}^{(1)} \text{ch}(\Gamma_{l1}^{(1)} x) + B_{l1}'^{(1)} \text{sh}(\Gamma_{l1}^{(1)} x) + B_{l1}^{(2)} \text{ch}(\Gamma_{l1}^{(2)} x) + B_{l1}'^{(2)} \text{sh}(\Gamma_{l1}^{(2)} x)] \sin(k_{y1} y)$$

$$E_{z1} = \frac{1}{j} \sum_{l=1}^{\infty} [D_{l1}^{(1)} \text{ch}(\Gamma_{l1}^{(1)} x) + D_{l1}'^{(1)} \text{sh}(\Gamma_{l1}^{(1)} x) + D_{l1}^{(2)} \text{ch}(\Gamma_{l1}^{(2)} x) + D_{l1}'^{(2)} \text{sh}(\Gamma_{l1}^{(2)} x)] \sin(k_{y1} y)$$

图 1 含铁氧体片的脊形波导模型($b > b'$)图 2 含铁氧体片的槽形波导模型($b < b'$)

$$H_{z1} = \frac{1}{j} [F_{01}^{(1)} \cos(k_{x01}^{(1)} x) + F_{01}^{'(1)} \sin(k_{x01}^{(1)} x)] + \frac{1}{j} \sum_{l=1}^{\infty} [F_{l1}^{(1)} \text{ch}(\Gamma_{l1}^{(1)} x) + F_{l1}^{'(1)} \text{sh}(\Gamma_{l1}^{(1)} x) + F_{l1}^{(2)} \text{ch}(\Gamma_{l1}^{(2)} x) + F_{l1}^{'(2)} \text{sh}(\Gamma_{l1}^{(2)} x)] \cos(k_{y1l} y)$$

上式中 $k_{y1l} = 2l\pi/b'$, $(k_{x01}^{(1)})^2 = -\beta^2 + \mu_{\perp} \epsilon_{r1} k_0^2$, $k_0^2 = \omega^2 \epsilon_0 \mu_0$, $\mu_{\perp} = (\mu^2 - \kappa^2)/\mu$,

$$(\Gamma_{l1}^{(1)})^2 = -\frac{1}{2} [r_{d1} + r_{hl1} + \sqrt{(r_{d1} - r_{hl1})^2 + 4\epsilon_{r1} k_0^2 (\frac{\kappa}{\mu} k_{y1l})^2}]$$

$$(\Gamma_{l1}^{(2)})^2 = -\frac{1}{2} [r_{d1} + r_{hl1} - \sqrt{(r_{d1} - r_{hl1})^2 + 4\epsilon_{r1} k_0^2 (\frac{\kappa}{\mu} k_{y1l})^2}]$$

$$r_{hl1} = -\frac{1}{\mu} k_{y1l}^2 - \beta^2 + \epsilon_{r1} k_0^2, r_{d1} = -k_{y1l}^2 - \beta^2 + \mu_{\perp} \epsilon_{r1} k_0^2, \quad l \geq 1$$

区域 2, 令 $x' = -x + a/2$, 则

$$E_{y2} = A_{02} \sin(k_{x02} x') + \sum_{l=1}^{\infty} A_{l2} \text{sh}(\Gamma_{l2} x') \cos(k_{y2l} y)$$

$$H_{y2} = \sum_{l=1}^{\infty} B_{l2} \text{ch}(\Gamma_{l2} x') \sin(k_{y2l} y)$$

$$E_{z2} = \frac{1}{j} \sum_{l=1}^{\infty} D_{l2} \text{sh}(\Gamma_{l2} x') \sin(k_{y2l} y)$$

$$H_{z2} = \frac{1}{j} F_{02} \cos(k_{x02} x') + \frac{1}{j} \sum_{l=1}^{\infty} F_{l2} \text{ch}(\Gamma_{l2} x') \cos(k_{y2l} y)$$

上式中 $k_{y2l} = 2l\pi/b$, $k_{x02}^2 = -\beta^2 + k_0^2$, $\Gamma_{l2}^2 = k_{y2l}^2 + \beta^2 - k_0^2$ ($l \geq 1$).

区域 3 中的场分为两种情况: (1) $x=0$ 为磁壁, 即 m 为奇数, 由“ l ”中的上式表示, (2) $x=0$ 为电壁, 即 m 为偶数, 由“ l ”中的下式表示.

$$E_{y3} = A_{03} \begin{bmatrix} \cos(k_{x03} x) \\ \sin(k_{x03} x) \end{bmatrix} + \sum_{l=1}^{\infty} A_{l3} \begin{bmatrix} \text{ch}(\Gamma_{l3} x) \\ \text{sh}(\Gamma_{l3} x) \end{bmatrix} \cos(k_{y3l} y)$$

$$H_{y3} = \sum_{l=1}^{\infty} B_{l3} \begin{bmatrix} \text{sh}(\Gamma_{l3} x) \\ \text{ch}(\Gamma_{l3} x) \end{bmatrix} \sin(k_{y3l} y)$$

$$E_{z3} = \frac{1}{j} \sum_{l=1}^{\infty} D_{l3} \begin{bmatrix} \text{ch}(\Gamma_{l3} x) \\ \text{sh}(\Gamma_{l3} x) \end{bmatrix} \sin(k_{y3l} y)$$

$$H_{z3} = \frac{1}{j} F_{03} \begin{bmatrix} \sin(k_{x03} x) \\ \cos(k_{x03} x) \end{bmatrix} + \frac{1}{j} \sum_{l=1}^{\infty} F_{l3} \begin{bmatrix} \text{sh}(\Gamma_{l3} x) \\ \text{ch}(\Gamma_{l3} x) \end{bmatrix} \cos(k_{y3l} y)$$

其中

$$k_{y3l} = k_{y1l}, k_{x03}^2 = -\beta^2 + \epsilon_{r3} k_0^2, \Gamma_{l3}^2 = k_{y3l}^2 + \beta^2 - \epsilon_{r3} k_0^2 (l \geq 1).$$

由波动方程确定的独立系数仅有 $A_{0l}^{(1)}$ 、 $A_{0l}^{'(1)}$ 、 $A_{l1}^{'(1)}$ 、 $A_{l1}^{(2)}$ 、 $A_{l1}^{'(2)}$ 、 A_{02} 、 A_{l2} 、 B_{l2} 、 A_{03} 、 A_{l3} 、 B_{l3} (系数间关系详见文献[4])。

2.3 各区域间边界条件匹配

区域 1、3 交界即 $x = \frac{c}{2}$ 处, 由切向场分量相等, 得

$$A_{01}^{(1)} \cos(k_{x01}^{(1)} \frac{c}{2}) + A_{01}^{'(1)} \sin(k_{x01}^{(1)} \frac{c}{2}) = A_{03}$$

$$\begin{bmatrix} \cos(k_{x03} \frac{c}{2}) \\ \sin(k_{x03} \frac{c}{2}) \end{bmatrix}$$

$$F_{01}^{(1)} \cos(k_{x01}^{(1)} \frac{c}{2}) + F_{01}^{'(1)} \sin(k_{x01}^{(1)} \frac{c}{2}) = F_{03}$$

$$\begin{bmatrix} \sin(k_{x03} \frac{c}{2}) \\ \cos(k_{x03} \frac{c}{2}) \end{bmatrix}$$

$$A_{l1}^{(1)} \text{ch}(\Gamma_{l1}^{(1)} \frac{c}{2}) + A_{l1}^{'(1)} \text{sh}(\Gamma_{l1}^{(1)} \frac{c}{2}) + A_{l1}^{(2)} \text{ch}(\Gamma_{l1}^{(2)} \frac{c}{2})$$

$$+ A_{l1}^{'(2)} \text{sh}(\Gamma_{l1}^{(2)} \frac{c}{2}) = A_{l3}$$

$$\begin{bmatrix} \text{ch}(\Gamma_{l3} \frac{c}{2}) \\ \text{sh}(\Gamma_{l3} \frac{c}{2}) \end{bmatrix}$$

$$B_{l1}^{(1)} \text{ch}(\Gamma_{l1}^{(1)} \frac{c}{2}) + B_{l1}^{'(1)} \text{sh}(\Gamma_{l1}^{(1)} \frac{c}{2}) + B_{l1}^{(2)} \text{ch}(\Gamma_{l1}^{(2)} \frac{c}{2})$$

$$+ B_{l1}^{'(2)} \text{sh}(\Gamma_{l1}^{(2)} \frac{c}{2}) = B_{l3}$$

$$\begin{bmatrix} \text{sh}(\Gamma_{l3} \frac{c}{2}) \\ \text{ch}(\Gamma_{l3} \frac{c}{2}) \end{bmatrix}$$

$$D_{l1}^{(1)} \text{ch}(\Gamma_{l1}^{(1)} \frac{c}{2}) + D_{l1}^{'(1)} \text{sh}(\Gamma_{l1}^{(1)} \frac{c}{2}) + D_{l1}^{(2)} \text{ch}(\Gamma_{l1}^{(2)} \frac{c}{2})$$

$$+ D_{l1}^{'(2)} \text{sh}(\Gamma_{l1}^{(2)} \frac{c}{2}) = D_{l3}$$

$$\begin{bmatrix} \text{ch}(\Gamma_{l3} \frac{c}{2}) \\ \text{sh}(\Gamma_{l3} \frac{c}{2}) \end{bmatrix}$$

$$F_{l1}^{(1)} \text{ch}(\Gamma_{l1}^{(1)} \frac{c}{2}) + F_{l1}^{'(1)} \text{sh}(\Gamma_{l1}^{(1)} \frac{c}{2}) + F_{l1}^{(2)} \text{ch}(\Gamma_{l1}^{(2)} \frac{c}{2})$$

$$+ F_{l1}^{'(2)} \text{sh}(\Gamma_{l1}^{(2)} \frac{c}{2}) = F_{l3}$$

$$\begin{bmatrix} \text{sh}(\Gamma_{l3} \frac{c}{2}) \\ \text{ch}(\Gamma_{l3} \frac{c}{2}) \end{bmatrix}$$

在区域 1、2 交界即 $x = a/2$ 处, 由于波导壁的突变, 边界条件不能处处匹配, 用伽辽金方法作近似处理.

(1) 对于槽波导, 注意到 $b/2 \leq |y| \leq b'/2$ 时, $x = a/2$ 处为电壁, $E_{y1} = E_{z1} = 0$. 用区域 1 的电场表示区域 2 的电场, 用区域 2 的磁场表示区域 1 的磁场, 令系数相等得:

$$a [A_{01}^{(1)} \cos(k_{x01}^{(1)} \frac{a}{2}) + A_{01}^{'(1)} \sin(k_{x01}^{(1)} \frac{a}{2})] = A_{02} \sin(k_{x02} \frac{a-a'}{2})$$

$$F_{01}^{(1)} \cos(k_{x01}^{(1)} \frac{a}{2}) + F_{01}^{'(1)} \sin(k_{x01}^{(1)} \frac{a}{2}) + \sum_{l=1}^{\infty} [F_{l1}^{(1)} \text{ch}(\Gamma_{l1}^{(1)} \frac{a}{2}) +$$

$$F_{l1}^{'(1)} \text{sh}(\Gamma_{l1}^{(1)} \frac{a}{2}) + F_{l1}^{(2)} \text{ch}(\Gamma_{l1}^{(2)} \frac{a}{2}) + F_{l1}^{'(2)} \text{sh}(\Gamma_{l1}^{(2)} \frac{a}{2})] J S(k_{y1l})$$

$$\begin{aligned} \frac{b}{2}) &= F_{02} \cos(k_{x0} \frac{a-a'}{2}) \\ \alpha [A_{p1}^{(1)} \operatorname{ch}(\Gamma_{p1}^{(1)} \frac{a'}{2}) + A_{p1}^{(1)} \operatorname{sh}(\Gamma_{p1}^{(1)} \frac{a'}{2}) + A_{p1}^{(2)} \operatorname{ch}(\Gamma_{p1}^{(2)} \frac{a'}{2}) + A_{p1}^{(2)} \\ \operatorname{sh}(\Gamma_{p1}^{(2)} \frac{a'}{2})] &= A_{02} \sin(k_{x02} \frac{a-a'}{2}) \cdot 2S(k_{yp1} \frac{b}{2}) + \sum_{l=1}^{\infty} A_{l2} \operatorname{sh}(\Gamma_{l2} \\ \frac{a-a'}{2}) \{ S[(k_{yp1} - k_{yl2}) \frac{b}{2}] + S[(k_{yp1} + k_{yl2}) \frac{b}{2}] \} \\ \sum_{l=1}^{\infty} B_{l1}^{(1)} \operatorname{ch}(\Gamma_{l1}^{(1)} \frac{a'}{2}) + B_{l1}^{(1)} \operatorname{sh}(\Gamma_{l1}^{(1)} \frac{a'}{2}) + B_{l1}^{(2)} \operatorname{ch}(\Gamma_{l1}^{(2)} \frac{a'}{2}) + \\ B_{l1}^{(2)} \operatorname{sh}(\Gamma_{l1}^{(2)} \frac{a'}{2}) \} & \{ S[(k_{yl1} - k_{yp2}) \frac{b}{2}] - S[(k_{yl1} + k_{yp2}) \frac{b}{2}] \} = \\ B_{p2} \operatorname{ch}(\Gamma_{p2} \frac{a-a'}{2}) \\ \alpha [D_{p1}^{(1)} \operatorname{ch}(\Gamma_{p1}^{(1)} \frac{a'}{2}) + D_{p1}^{(1)} \operatorname{sh}(\Gamma_{p1}^{(1)} \frac{a'}{2}) + D_{p1}^{(2)} \operatorname{ch}(\Gamma_{p1}^{(2)} \frac{a'}{2}) + \\ D_{p1}^{(2)} \operatorname{sh}(\Gamma_{p1}^{(2)} \frac{a'}{2})] &= \sum_{l=1}^{\infty} D_{l2} \operatorname{sh}(\Gamma_{l2} \frac{a-a'}{2}) \{ S[(k_{yp1} - k_{yl2}) \frac{b}{2}] - \\ S[(k_{yp1} + k_{yl2}) \frac{b}{2}] \} \\ \sum_{i=1}^{\infty} F_{i1}^{(1)} \operatorname{ch}(\Gamma_{i1}^{(1)} \frac{a'}{2}) + F_{i1}^{(1)} \operatorname{sh}(\Gamma_{i1}^{(1)} \frac{a'}{2}) + F_{i1}^{(2)} \operatorname{ch}(\Gamma_{i1}^{(2)} \frac{a'}{2}) + \\ F_{i1}^{(2)} \operatorname{sh}(\Gamma_{i1}^{(2)} \frac{a'}{2}) \} & \{ S[(k_{yl1} - k_{yp2}) \frac{b}{2}] + S[(k_{yl1} + k_{yp2}) \frac{b}{2}] \} = \\ F_{p2} \operatorname{ch}(\Gamma_{p2} \frac{a-a'}{2}) \end{aligned}$$

(2) 对于脊波导, 注意到 $\frac{b'}{2} \leq |y| \leq \frac{b}{2}$ 时, $x = \frac{a'}{2}$ 处为电壁, $E_{y2} = E_{z2} = 0$. 用区域 2 的电场表示区域 1 的电场, 用区域 1 的磁场表示区域 2 的磁场, 令系数相等得:

$$\begin{aligned} \alpha [A_{01}^{(1)} \cos(k_{x01} \frac{a'}{2}) + A_{01}^{(1)} \sin(k_{x01} \frac{a'}{2})] &= A_{02} \sin(k_{x02} \frac{a-a'}{2}) \\ F_{01}^{(1)} \cos(k_{x01} \frac{a'}{2}) + F_{01}^{(1)} \sin(k_{x01} \frac{a'}{2}) &= F_{02} \cos(k_{x02} \frac{a-a'}{2}) + \\ \sum_{l=1}^{\infty} F_{l2} \operatorname{ch}(\Gamma_{l2} \frac{a-a'}{2}) S(k_{yl2} \frac{b'}{2}) \\ [A_{01}^{(1)} \cos(k_{x01} \frac{a'}{2}) + A_{01}^{(1)} \sin(k_{x01} \frac{a'}{2})] \cdot 2\alpha S(k_{yp2} \frac{b'}{2}) + \sum_{l=1}^{\infty} [A_{l1}^{(1)} \\ \operatorname{ch}(\Gamma_{l1}^{(1)} \frac{a'}{2}) + A_{l1}^{(1)} \operatorname{sh}(\Gamma_{l1}^{(1)} \frac{a'}{2}) + A_{l1}^{(2)} \operatorname{ch}(\Gamma_{l1}^{(2)} \frac{a'}{2}) + A_{l1}^{(2)} \operatorname{sh}(\Gamma_{l1}^{(2)} \frac{a'}{2})] \end{aligned}$$

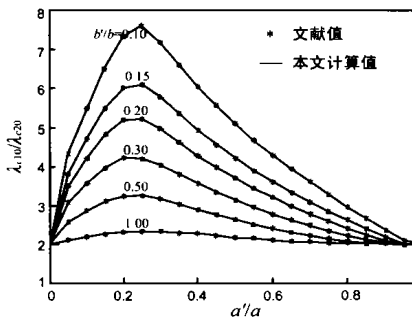


图 3 脊形波导的带宽特性

3.2 填充铁氧体片的矩形波导

即 $b = b'$ 情形, 这时高次模消失, $H_y = E_z = 0$, 主模为 TE₁₀ 模. 图 4 给出工作频率 $f_0 = 10\text{GHz}$, $a = 0.761\lambda_0$, $b = 0.33\lambda_0$, ϵ_r

$$\begin{aligned} \frac{a'}{2}) \cdot \alpha \{ S[(k_{yl1} - k_{yp2}) \frac{b'}{2}] + S[(k_{yl1} + k_{yp2}) \frac{b'}{2}] \} &= A_{p2} \operatorname{sh}(\Gamma_{p2} \\ \frac{a-a'}{2}) \\ B_{p1}^{(1)} \operatorname{ch}(\Gamma_{p1}^{(1)} \frac{a'}{2}) + B_{p1}^{(1)} \operatorname{sh}(\Gamma_{p1}^{(1)} \frac{a'}{2}) + B_{p1}^{(2)} \operatorname{ch}(\Gamma_{p1}^{(2)} \frac{a'}{2}) + B_{p1}^{(2)} \operatorname{sh} \\ (\Gamma_{p1}^{(2)} \frac{a'}{2}) &= \sum_{l=1}^{\infty} B_{l2} \operatorname{ch}(\Gamma_{l2} \frac{a-a'}{2}) \{ S[(k_{yp1} - k_{yl2}) \frac{b}{2}] - S[(k_{yp1} \\ + k_{yl2}) \frac{b}{2}] \} \\ \sum_{l=1}^{\infty} [D_{l1}^{(1)} \operatorname{ch}(\Gamma_{l1}^{(1)} \frac{a'}{2}) + D_{l1}^{(1)} \operatorname{sh}(\Gamma_{l1}^{(1)} \frac{a'}{2}) + D_{l1}^{(2)} \operatorname{ch}(\Gamma_{l1}^{(2)} \frac{a'}{2}) + \\ D_{l1}^{(2)} \operatorname{sh}(\Gamma_{l1}^{(2)} \frac{a'}{2})] \\ \cdot \alpha \{ S[(k_{yl1} - k_{yp2}) \frac{b'}{2}] - S[(k_{yl1} + k_{yp2}) \frac{b'}{2}] \} &= D_{p2} \operatorname{sh}(\Gamma_{p2} \\ \frac{a-a'}{2}) \\ F_{p1}^{(1)} \operatorname{ch}(\Gamma_{p1}^{(1)} \frac{a'}{2}) + F_{p1}^{(1)} \operatorname{sh}(\Gamma_{p1}^{(1)} \frac{a'}{2}) + F_{p1}^{(2)} \operatorname{ch}(\Gamma_{p1}^{(2)} \frac{a'}{2}) + F_{p1}^{(2)} \operatorname{sh} \\ (\Gamma_{p1}^{(2)} \frac{a'}{2}) &= \sum_{l=1}^{\infty} F_{l2} \operatorname{ch}(\Gamma_{l2} \frac{a-a'}{2}) \{ S[(k_{yp1} - k_{yl2}) \frac{b}{2}] + S \\ [(k_{yp1} + k_{yl2}) \frac{b}{2}] \} \\ \text{上式中 } S(x) &= \frac{\sin x}{x}, \alpha = \frac{b'}{b}. \end{aligned}$$

若取 L 个高次模, 边界条件为含有 $4 + 8L$ 个未知数的齐次方程组. 令系数行列式为零, 结合特征方程, 可求出截止频率, 相位常数和相位移等.

3 计算结果

3.1 填充非均匀介质的脊形波导

即 $c = a'$ 情形, 这时区域 1 消失. 图 3 给出 $b/a = 0.5$, $\epsilon_r = 2.05$ 时, 准 TE₁₀ 模的带宽特性随波导尺寸变化的曲线, 与文献[1] Fig2(b) 吻合. 文献[1] 假设传输模式是 TE_{m0} 模, 在脊形波导中实际是不存在的. 但由 TE_{m0} 模所求截止频率与本文相应的混合模式准 TE_{m0} 模的截止频率相同, 说明文献[1] 的方法在求截止频率时是可行的.

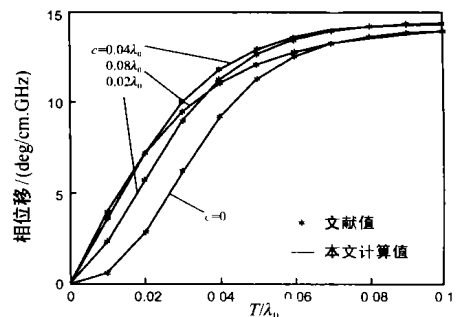


图 4 矩形波导相位移与铁氧体片厚度关系

$= 12$, $\kappa = 0.8$, $\epsilon_r = 13$ 时, TE₁₀ 模的相位移与铁氧体片厚度 ($T = \frac{a' - c}{2}$) 关系曲线, 与文献[2] Fig4 吻合.

3.3 填充铁氧体片的槽形、脊形波导

图 5(a)、(b) 给出中心频率 $f_0 = 10\text{GHz}$, $a = 0.724\lambda_0$, $b' = 0.323\lambda_0$, $\epsilon_r = 12$, $\kappa = 0.5186$, $\epsilon_r = 13$ 时槽形波导主模准 TE₁₀ 模的相位移与波导高度、工作频率关系曲线。L 取 0 时, 仅考虑基模, 即文献[3]的方法, 此时计算曲线为图中虚线。实线 L 取 4, 考虑 4 阶高次模。当 b 与 b' 相差很小时, 虚线与实线接近; 反之, 虚线与实线相差很大, 而实线更接近于实际, 这说明

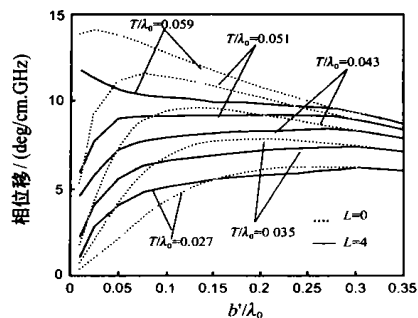


图 5 (a) 槽形波导相位移与波导高度关系 ($c = 0.04\lambda_0, f = f_0$)

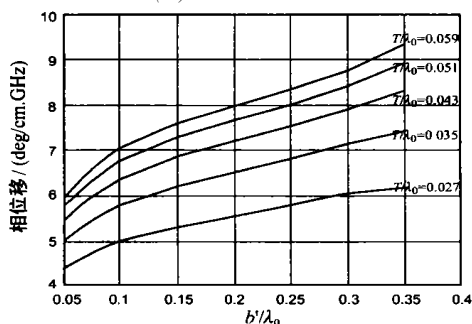
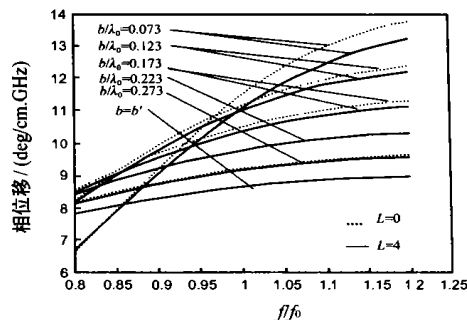


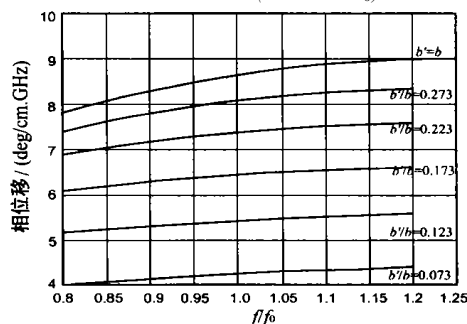
图 6 (a) 脊形波导相位移与波导高度之间关系 ($c = 0.04\lambda_0, f = f_0$)

当 b 与 b' 相差较大时, 高次模的影响不可忽略。

图 6(a)、(b) 给出 $f_0 = 10\text{GHz}$, $a = 0.724\lambda_0$, $b = 0.323\lambda_0$, $\epsilon_r = 12$, $\kappa = 0.5186$, $\epsilon_r = 13$, L 取 4 时脊形波导主模的相位移与波导高度、工作频率关系曲线。比较图 5 与图 6 可见, 槽形波导具有较大相位移, 而脊形波导具有宽频带特性。



(b) 脊形波导相位移与频率关系 ($T = 0.051\lambda_0$)



(b) 脊形波导相位移与频率关系 ($T = 0.051\lambda_0$)

4 结论

本文首次精确给出了含铁氧体片的脊形和槽形波导中的传输模式。3.1、3.2 节计算了填充非均匀介质的脊形波导的频率特性和含铁氧体片的矩形波导的相位移特性, 与文献[1, 2]比较, 结果吻合, 说明此方法的可靠性。3.3 计算了槽形波导与脊形波导的相位移特性, 得出与相差较大时高次模的影响很大, 考虑高次模结果更精确。计算结果表明含铁氧体片的脊形波导具有宽频带特性, 含铁氧体片的槽形波导具有较大相位移。

参考文献:

- [1] G Magerl. Ridged waveguides with inhomogeneous dielectric slab loading [J]. IEEE Trans, 1978, MTT-26(6): 413-416.
- [2] W J Ince, E Stem. Nonreciprocal remanence phase shifters in rectangular waveguide [J]. IEEE Trans, 1967, MTT-15(2): 87-95.
- [3] A Mizobuchi, H Kurebayashi. Nonreciprocal remanence ferrite phase shifters using the grooved waveguide [J]. IEEE Trans, 1978, MTT-26(12): 1012-1016.
- [4] 宗卫华. 含铁氧体片的脊(槽)形波导传输特性 [D]. 南京: 南京电子工程研究中心, 2000. 8-13.
- [5] M Okoniewski, J Mazur. An accurate field matching analysis of waveguides of complex cross sectional geometry loaded with magnetized ferrite rods [J]. IEEE Trans, 1995, MTT-43(4): 880-886.

作者简介:



宗卫华 女, 1975 年生于山东蓬莱, 1997 年 7 月毕业于烟台大学数学系, 获理学学士学位, 2000 年 3 月毕业于南京电子工程研究中心电磁场与微波技术专业, 获工学硕士学位, 现在西安电子科技大学电磁场与微波技术专业攻读博士学位。目前主要从事于电磁场的数值计算及电磁兼容方面的研究。

余显烨

(1938-2000) 男, 生于上海, 1960 年毕业于北京大学数力系, 其后一直在南京电子技术研究所工作。1983 年 1 月~1985 年 7 月在加拿大滑铁卢大学做访问学者。出版专著 3 本, 发表论文 50 余篇。



梁昌洪 男, 1943 年生于上海, 现为西安电子科技大学校长, 教授, 博士生导师, 并为中国电子学会会士, IEEE 高级会员。研究方向包括计算场论、计算微波、微波网络理论、近代数据处理、电磁散射与逆散射。